Supplement of

Development and application of a multi-scale modelling framework for urban high-resolution NO_2 pollution mapping

Zhaofeng Lv[★], Zhenyu Luo[★], Fanyuan Deng, Xiaotong Wang, Junchao Zhao, Lucheng Xu, Tingkun He, Huan Liu*, Kebin He
State Key Joint Laboratory of ESPC, School of Environment, Tsinghua University, Beijing 100084, China
[★]Z. Lv. and Z. Luo. contributed equally to this work.
Corresponding Author:
*Phone and fax: 86-10-62771679; e-mail: liu_env@tsinghua.edu.cn.

Supplementary Figures

Figure S1. Spatial distribution of street canyon geometry in Beijing (© Microsoft). (a) Length of actual street canyon to the total street length, (b) Height to width ratio, (c) Length to height ratio and (d) Height symmetrical ratio.

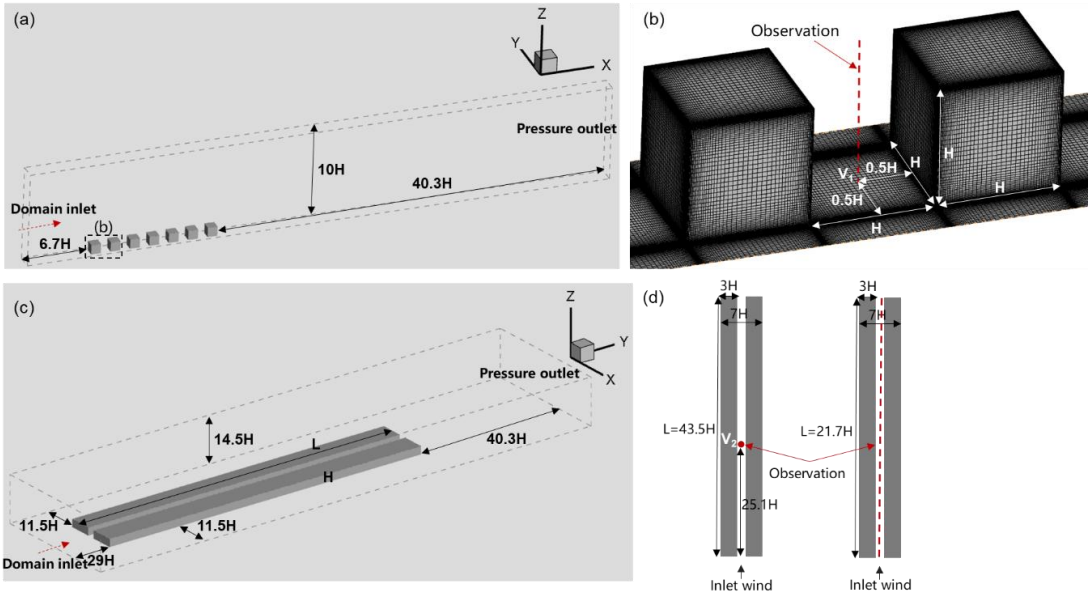

Figure S2. Computational domain and grid arrangement in CFD validation cases with the background wind being perpendicular (a-b) or parallel (c-d) to the axis of street canyons. In the first validation case (a-b), the vertical profiles of time-averaged velocity components (stream-wise velocity U and vertical velocity W) are measured at point V_1. In another validation case (c-d), the vertical (point V_2) and horizontal (z=0.11H) profiles of time-averaged stream-wise velocity U are measured.

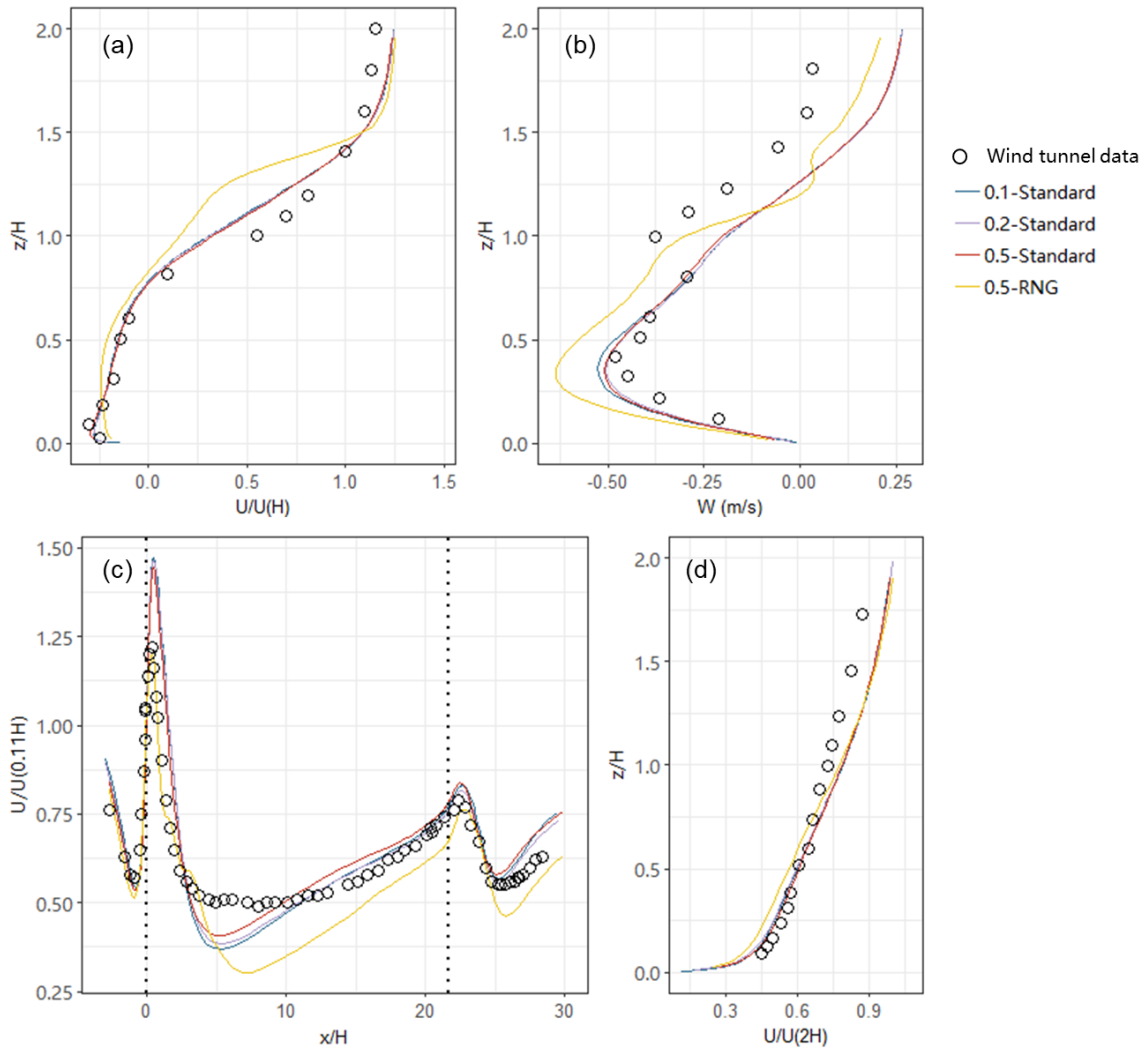

Figure S3. Model performances of CFD validation cases in street canyons perpendicular (a-b) or parallel (c-d) to the wind direction at the roof level. (a) Vertical profiles of U at point V_1; (b) Vertical profiles of W at point V_1; (c) Horizontal profiles of U at z=0.11H; (b) Vertical profiles of U at point V_2. In each validation case, three grid arrangement are tested, where the minimum sizes of hexahedral cells near wall surfaces are 0.1 m (fine grid), 0.2 m (medium grid) and 0.5 m (coarse grid) respectively. Moreover, the standard and RNG k-ε turbulence models are tested respectively.

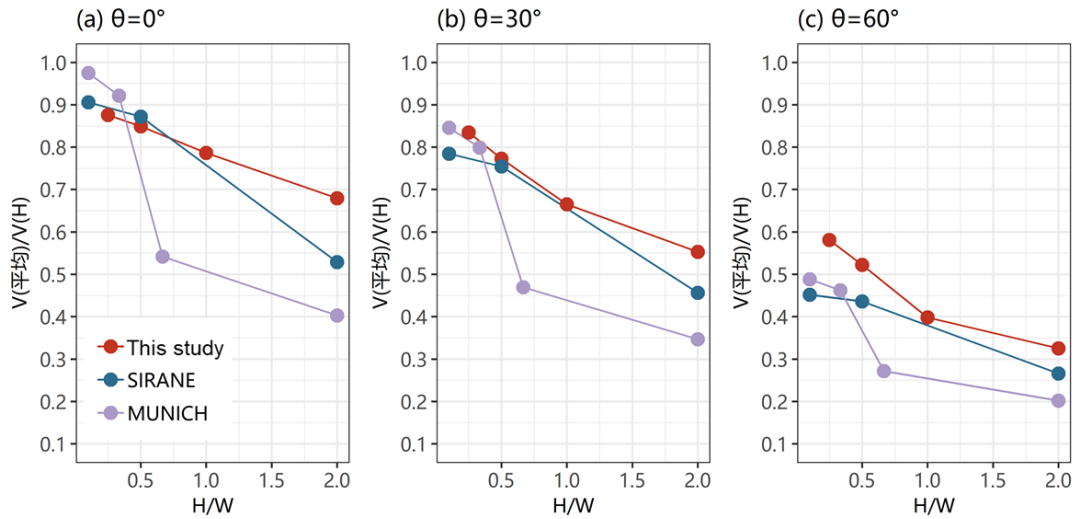

Figure S4. Comparison between the predicted wind speed in street canyons with different background wind direction and aspect ratio and other research results.

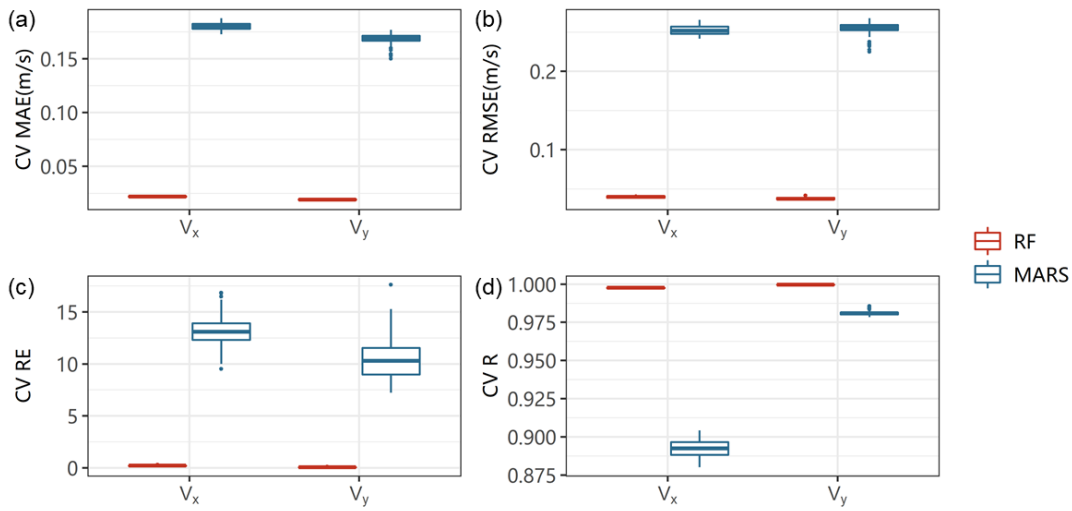

Figure S5. Model performance statistics of machine learning for $\boldsymbol{V_x}$ and $\boldsymbol{V_y}$ in street canyon. (a) MAE; (b) RMSE; (c) RE; (d) R.

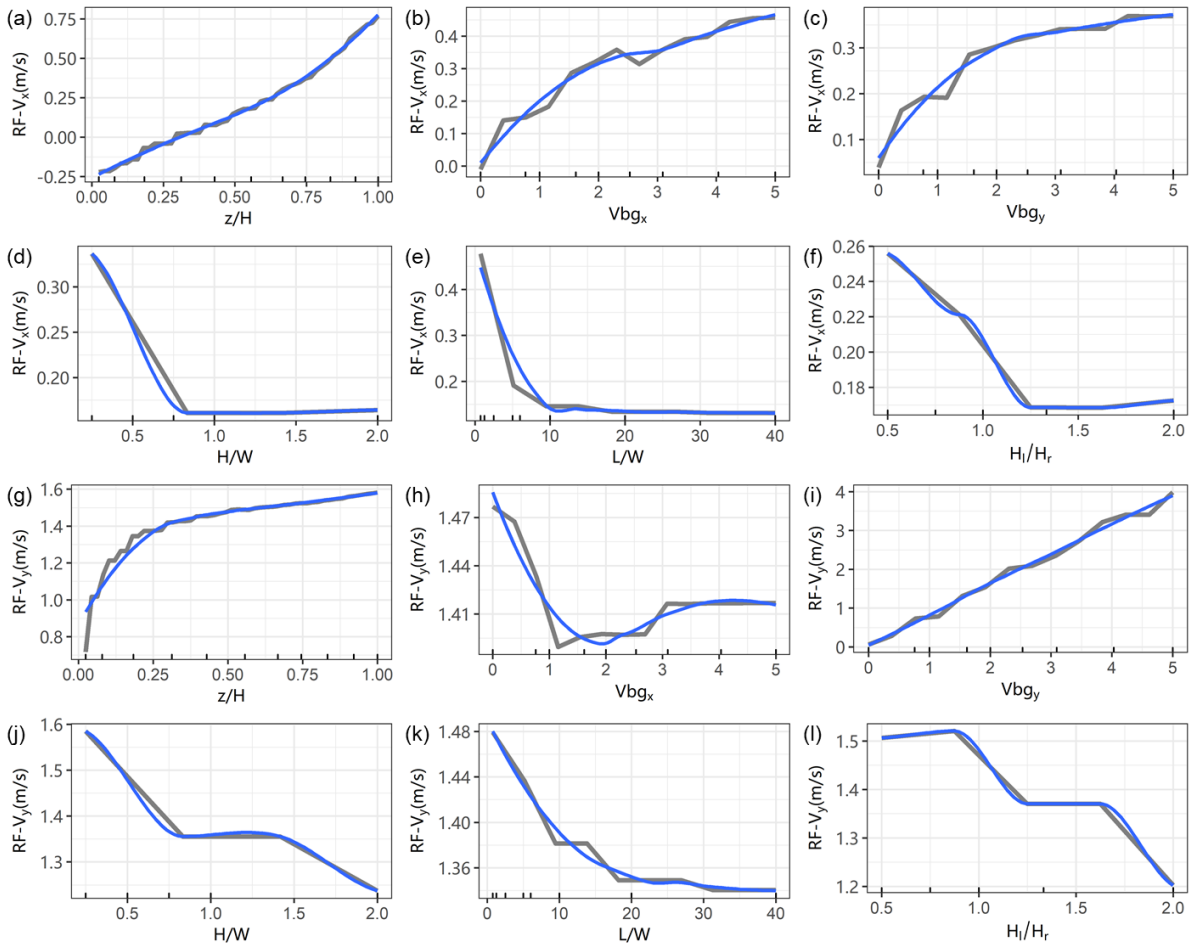

Figure S6. The partial dependence plots of each predictor variable in RF model for V_x (a-f) and V_y (g-l). The blue line stands for the smooth fitting curves. The labels above the x-axis shows deciles, minimum and maximum of the predictor variable.

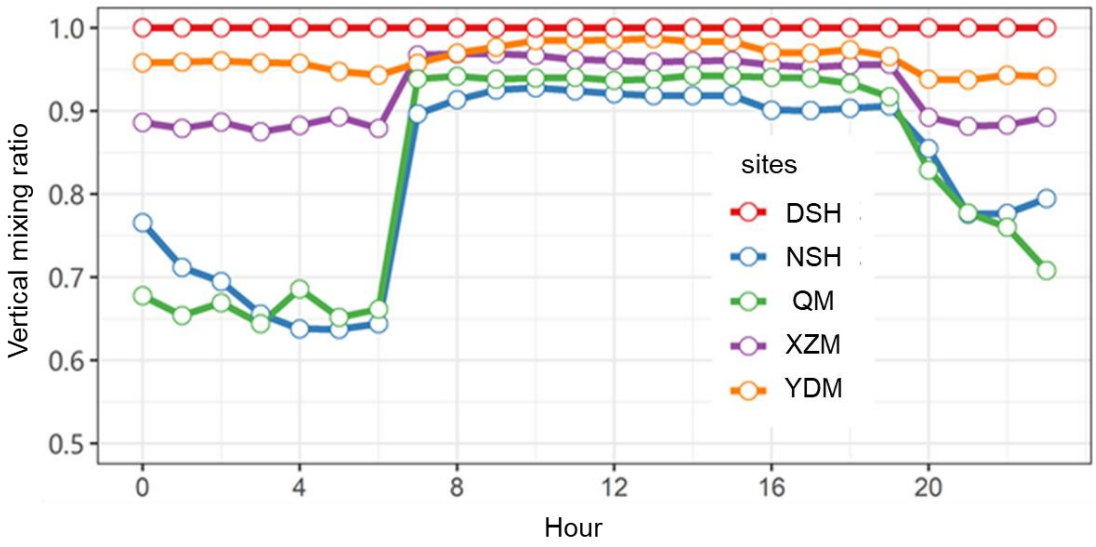

Figure S7. Diurnal variation of background concentration mixing ratio at roadside monitoring sites in Beijing in summer 2019. The vertical mixing ratio=concentrations near surface/at the top of UCL

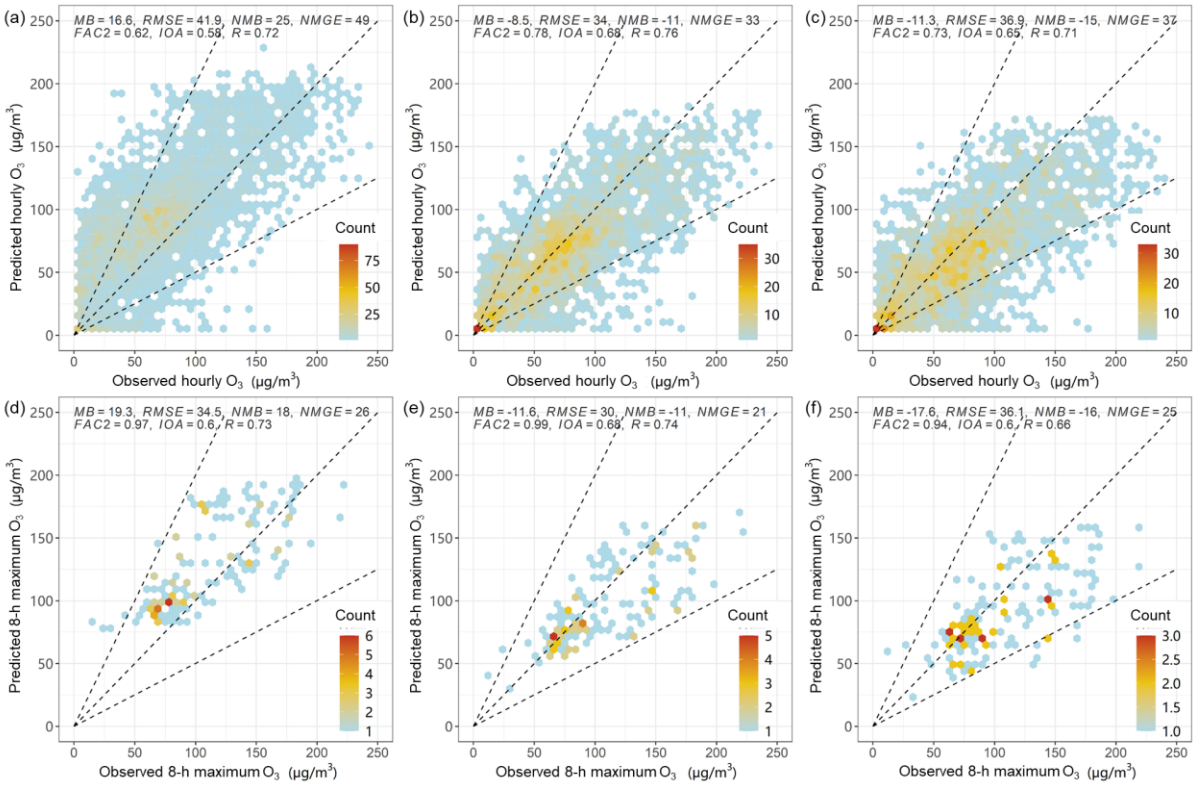

Figure S8. Observed and predicted hourly (a-c) or 8-h maximum averaged (d-f) O_3 concentrations from different models at near-road sites: (a, d) CMAQ model; (b, e) CMAQ-RLINE model; (c, f) CMAQ-RLINE_URBAN model.

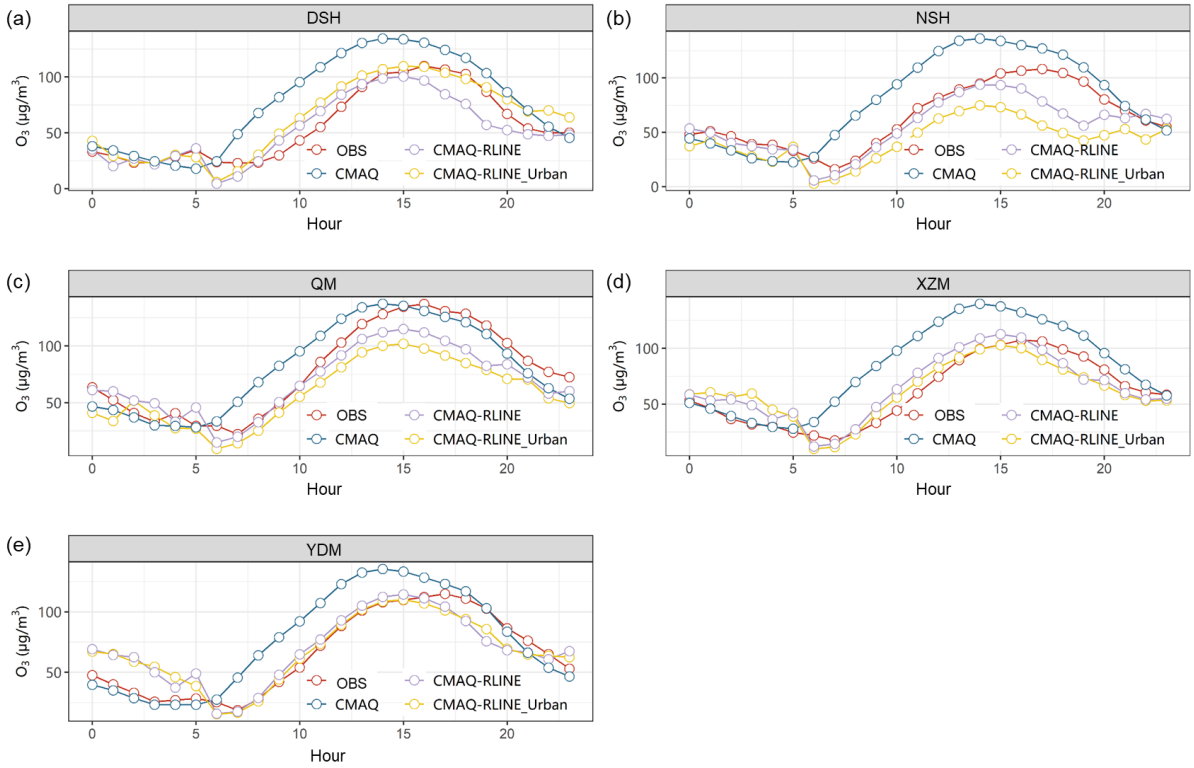

Figure S9. Diurnal variations of observed and predicted hourly averaged O_3 concentrations from different models at near-road monitoring sites: (a) DSH; (b) NSH; (c) QM; (d) XZM; (e) YDM.

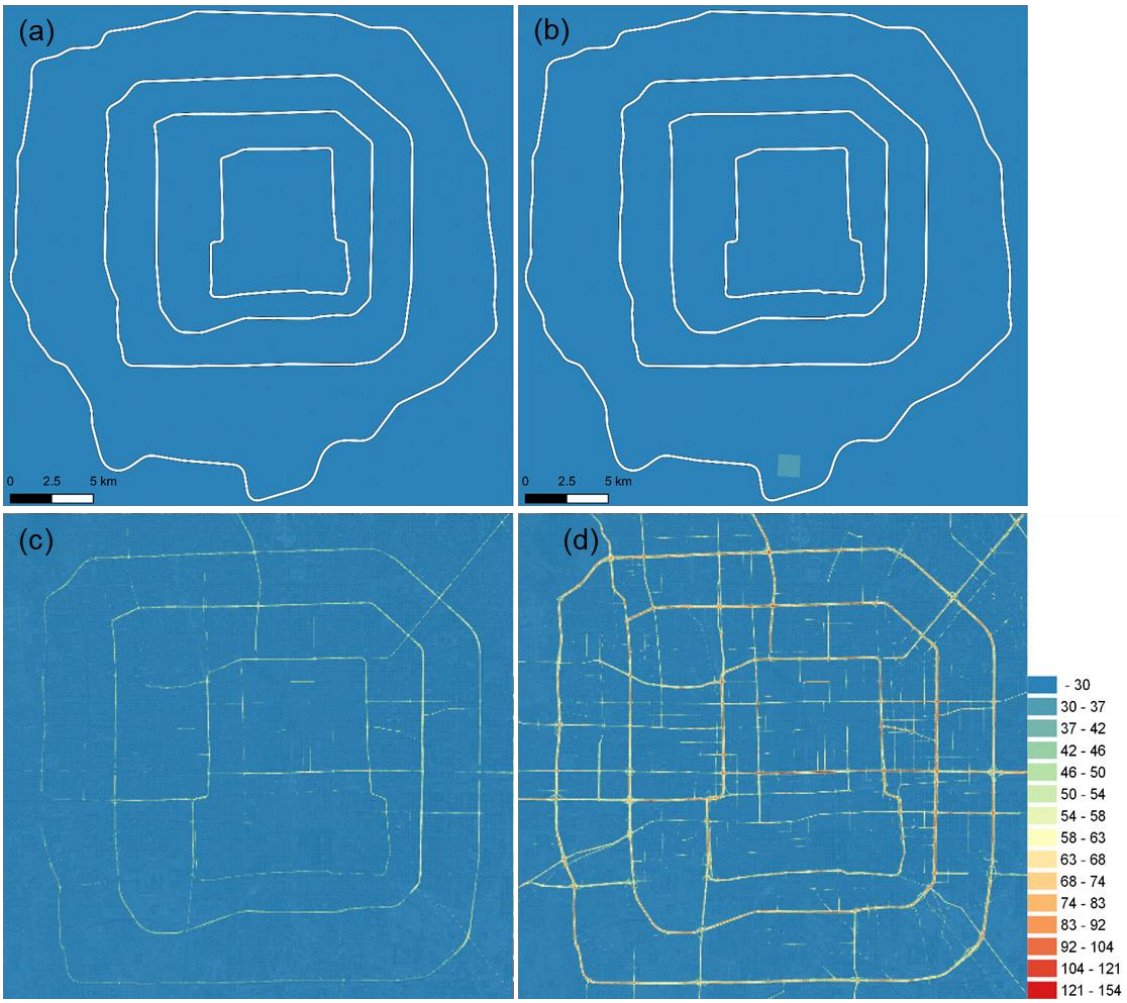

Figure S10. Spatial distribution of hourly averaged NO_2 concentrations from (a, b) CMAQ model and (c, d) CMAQ-RLINE_URBAN model at (a, c)12:00-13:00 and (b, d) 18:00-19:00.

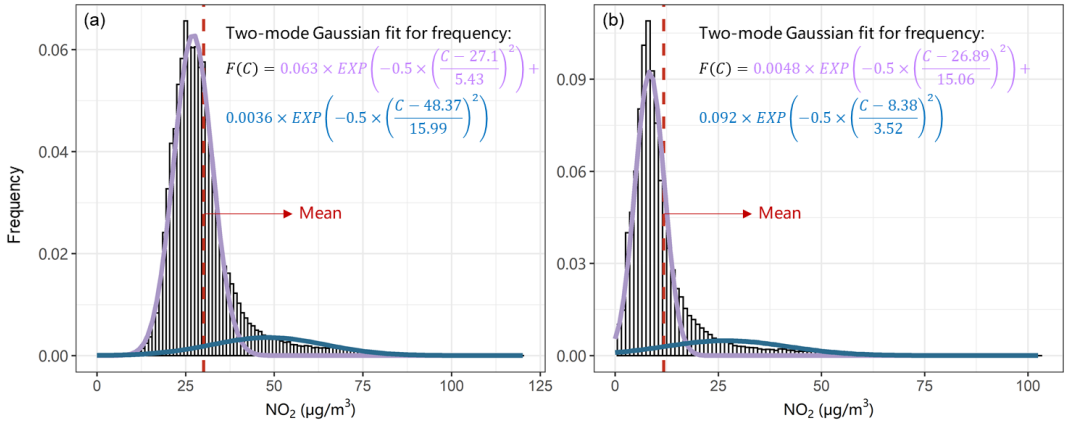

Figure S11. Frequency distribution of predicted monthly averaged NO2 concentrations from (a) all source and (b) only vehicles. Two-mode Gaussian models, which are shown by purple and blue curves, are used to fit for the distribution.

Supplementary Tables

Table S1. Model performance statistics for the velocity components in CFD validation cases.

Species	Mean Observation (m/s)	Mean Simulation (m/s)	FAC2	MFB (%)	NMSE (%)	R
Validation case with the perpendicular background wind						
u	-0.48	-0.50	1.00	-5	2	0.98
w	-0.37	-0.39	1.00	-4	5	0.58
Validation case with the parallel background wind						
u(L=21.7H)	0.68	0.73	1.00	-7	3	0.97
u(L=43.5H)	0.58	0.59	1.00	-1	0	0.99

Note: The coarse grid arrangement and standard k-ε turbulence model are used.
*MFB: Mean fractional

Table S2. Geometric characters for each monitoring site

Stations	*H*/*W*	bd	bh（m）	bhsd（m）	z_0（m）
DSH	0	0.01	4.97	1.68	1
NSH	0	0.13	19.61	31.96	1.06
QM	0.22	0.2	9.98	3.56	1.37
XZM	0.35	0.18	14.11	16.22	2.11
YDM	0	0.22	10.13	4.55	1.02

**H/W*, bd, bh, bhsd, and z_0 represent street canyon aspect ratio, average building height (m), height standard deviation (m) and plane density, respectively (Benavides et al., 2019).

Table S3. Model performances under different scenarios for each station

Sites	Scenario	MB	RMSE	NMB	NMGE	FAC2	IOA	*R*
	CMAQ	-15.6	33.4	-28	48	0.53	0.45	0.52
DSH	CMAQ-RLINE	28.2	63.1	51	69	0.73	0.20	0.50
	CMAQ-RLINE_URBAN	-6.2	28.5	-11	36	0.84	0.58	0.60
	CMAQ	-20.5	37.9	-33	50	0.53	0.12	0.30
NSH	CMAQ-RLINE	30.2	65.1	49	65	0.76	-0.12	0.33
	CMAQ-RLINE_URBAN	17.2	39.8	28	48	0.81	0.15	0.28
	CMAQ	-6.0	23.9	-14	42	0.64	0.45	0.59
QM	CMAQ-RLINE	20.4	55.2	47	68	0.8	0.11	0.47
	CMAQ-RLINE_URBAN	3.5	23.7	8	38	0.86	0.50	0.47
	CMAQ	-8.5	25.3	-18	44	0.61	0.36	0.54
XZM	CMAQ-RLINE	26.0	59.7	56	72	0.76	-0.06	0.41
	CMAQ-RLINE_URBAN	11.3	28.0	24	44	0.86	0.36	0.42
	CMAQ	0.6	25.5	1	44	0.66	0.43	0.58
YDM	CMAQ-RLINE	23.0	56.2	53	73	0.72	0.05	0.45
	CMAQ-RLINE_URBAN	5.4	25.0	12	39	0.86	0.50	0.50

*MB: Mean bias; RSME: Root mean squared error; NMB: Normalized mean bias; NMGE: Normalized mean gross error; FAC2: Fraction of predictions within a factor of two; IOA: Index of agreement; R: correlation coefficient.

Reference

Benavides, J., Snyder, M., Guevara, M., Soret, A., Pérez García-Pando, C., Amato, F., Querol, X., and Jorba, O.: CALIOPE-Urban v1.0: coupling R-LINE with a mesoscale air quality modelling system for urban air quality forecasts over Barcelona city (Spain), Geosci. Model Dev., 12, 2811-2835, 10.5194/gmd-12-2811-2019, 2019.